Mol Genet Genomics (2007) 277:171–188
DOI 10.1007/s00438-006-0182-0

ORIGINAL PAPER

The transcription factor Gcr1 stimulates cell growth by participating in nutrient-responsive gene expression on a global level

Kellie E. Barbara · Terry M. Haley · Kristine A. Willis · George M. Santangelo

Received: 3 September 2006 / Accepted: 6 October 2006 / Published online: 24 November 2006

Abstract Transcriptomic reprogramming is critical to the coordination between growth and cell cycle progression in response to changing extracellular conditions. In *Saccharomyces cerevisiae*, the transcription factor Gcr1 contributes to this coordination by supporting maximum expression of G1 cyclins in addition to regulating both glucose-induced and glucose-repressed genes. We report here the comprehensive genome-wide expression profiling of *gcr1*Δ cells. Our data show that reduced expression of ribosomal protein genes in *gcr1*Δ cells is detectable both 20 min after glucose addition and in steady-state cultures of raffinose-grown cells, showing that this defect is not the result of slow growth or growth on a repressing sugar. However, the large cell phenotype of the *gcr1*Δ mutant occurs only in the presence of repressing sugars. *GCR1* deletion also results in aberrant derepression of numerous glucose repressed loci; glucose-grown *gcr1*Δ cells actively respire, demonstrating that this global alteration in transcription corresponds to significant changes at the physiological level. These data offer an insight into the coordination of growth and cell division by providing an integrated view of the transcriptomic, phenotypic, and metabolic consequences of *GCR1* deletion.

Communicated by S. Hohmann.

K. E. Barbara · T. M. Haley · K. A. Willis · G. M. Santangelo (✉)
Mississippi Functional Genomics Network,
The University of Southern Mississippi,
118 College Dr., Hattiesburg, MS, USA
e-mail: GMS@mfgn.usm.edu

Keywords Glycolysis · Ribosomal proteins · *YBR187W* · Respiration · Cell size · Reverse recruitment

Introduction

The budding yeast *Saccharomyces cerevisiae* has been widely used as a model organism to study the proliferative response to nutrients in eukaryotic cells. Networked processes in *S. cerevisiae* that contribute to this response include energy metabolism, protein biosynthesis, cell cycle progression, and gene regulation. Precise coordination of these processes is a critical feature of the extraordinary capacity of yeast cells to adjust the rate of cell division rapidly in response to nutritional changes. For example, the *S. cerevisiae* transcriptome undergoes a dynamic reprogramming (Wang et al. 2004) within minutes of the appearance of its preferred carbon source (C-source), glucose (Polakis and Bartley 1966). Glucose addition down-regulates expression of genes involved in utilization of reserve carbohydrates, catabolism of alternative C-sources, and respiration; a nearly comprehensive wiring diagram of this glucose repression regulatory pathway (Santangelo 2006), which can also be triggered by the fermentable sugar galactose (Polakis and Bartley 1965), is now available. Glucose-dependent repression is accompanied by simultaneous up-regulation of genes required for rapid energy production, growth, and cell cycle progression; these genes encode glycolytic enzymes, ribosomal proteins, and cyclins, respectively (Deminoff et al. 2003; Santangelo 2006).

Faster cell division upon the appearance of glucose requires careful coordination of growth with cell cycle

progression (Hartwell 1974). This coordination occurs at Start in the G1 phase of the cell cycle, which is the gating event regulating the commitment to begin each new round of cell division (Hartwell et al. 1974). Numerous inputs contribute to timely passage through Start, including attainment of a critical cell size (Johnston et al. 1977), ample nutrient supply (Hartwell et al. 1974), and a critical rate of protein synthesis (Popolo et al. 1982). Impaired coordination between the cell and growth cycles causes division to occur at an abnormal size. For instance, mutations that cause premature passage through Start yield smaller cells (collectively called *whi* mutants). Conversely, mutations that delay passage through Start yield larger cells (collectively called *lge* mutants). Genome-wide cell size analysis of the yeast haploid knockout collection (Jorgensen et al. 2002) has identified ~500 genes which, when deleted, cause a *whi* or *lge* phenotype. Many of these genes encode specific cell cycle regulators such as the well-characterized G1 cyclins (Cln1, Cln2, and Cln3) that are required for the transition at Start; other cellular processes, including protein synthesis and regulation of RNA polymerase II transcription, are also well-represented (Jorgensen et al. 2002).

Gcr1, a global regulator of RNA polymerase II transcription (Menon et al. 2005; Santangelo 2006), is required for normal glucose induction of the G1 cyclin genes, *CLN1-3* (Parviz and Heideman 1998; Willis et al. 2003); in the absence of *GCR1*, *CLN* transcription is reduced, glucose-grown cells are much larger than their wild type counterparts, and a greater percentage of cells are unbudded due to a G1 delay in the cell cycle (Willis et al. 2003). Transcription of glycolytic and ribosomal protein genes (RPGs) is also impaired in *gcr1*Δ cells (Clifton and Fraenkel 1981; Santangelo and Tornow 1990; Tornow et al. 1993; Zeng et al. 1997; Deminoff and Santangelo 2001). Thus the Gcr1 regulator appears to target each of the predominant gene classes that are up-regulated in faster dividing glucose-grown cells (see above). Control of these genes appears to represent the fulcrum of growth/cell cycle coordination. Recent work has indicated that Gcr1 also contributes to glucose repression (Turkel et al. 2003; Sasaki and Uemura 2005). Indeed, derepression of genes normally repressed by glucose is essential in the absence of Gcr1; it is not possible to isolate *gcr1*Δ cells that are ρ^- or ρ^0 (i.e., that lack functional mitochondria; our unpublished data). Both the activator and repressor functions of Gcr1 are proposed to operate through a recently discovered nuclear-pore mediated mechanism termed reverse recruitment (Menon et al. 2005; Santangelo 2006; and our unpublished data).

We report here an analysis of the phenotypic, transcriptomic, and metabolic consequences of Gcr1 removal in the presence of various C-sources: fermentable repressing sugars (glucose and galactose), a non-repressing fermentable sugar (raffinose), and a non-fermentable C-source (pyruvate). We found that growth of *gcr1*Δ cells is defective in all C-sources tested. Interestingly however, the *lge* phenotype of *gcr1*Δ cells requires the presence of a repressing sugar. We used genome-wide expression profiling to comprehensively identify loci that exhibit defective transcription in *gcr1*Δ cells irrespective of C-source; this analysis identified both previously known and novel Gcr1 targets. Using an established method for separating regulated changes in the transcriptional program of the cell from metabolic changes induced by glucose (Wang et al. 2004), we verified that the defect we observed in RPG expression in *gcr1*Δ cells is independent of both growth rate and glucose metabolism. Our genomic analysis also detected loci whose expression was increased in *gcr1*Δ cells; as expected, this includes a significant number of normally glucose-repressed genes. Respiration-dependent staining of mitochondria confirmed at the metabolic level that Gcr1, in addition to activating glucose-induced genes, is also required for glucose repression of mitochondrial function.

Materials and methods

Strains and growth conditions

Isogenic *S. cerevisiae* wild type [BY263, Mat a *ade2-107 his3Δ200 leu2-Δ1 trp1*Δ63 *ura3-52 lys2-80* (Measday et al. 1994)], *gcr1*Δ [KW1433, same as BY263 except *gcr1*::*URA* (Willis et al. 2003)], and *cln3*Δ [GMS3503, same as BY263 except *cln3*::*URA3* (Willis et al. 2003)] strains (S288C background) were used in this study. All strains were grown at 23°C (due to the temperature sensitive phenotype of the *gcr1*Δ mutant; Willis et al. 2003) as batch cultures in YEP containing the indicated C-sources. A Beckman Coulter MultiSizer 3.0 was used to measure cell density (cells/ml) and cell volume (fl); each growth curve was derived from three independent experiments. Mitochondrial staining was done on cells grown to mid-logarithmic phase in the C-source indicated.

Transcriptomic analysis

Steady-state microarray analyses were done by isolating total RNA (Wang et al. 2004) from isogenic *gcr1*Δ and wild type cultures grown to early logarithmic

phase. Time course microarrays to analyze the immediate response to glucose were done by growing the same two strains in YEP containing 3% pyruvate as the carbon source. A reference sample was taken immediately prior to the addition of glucose (time zero); further aliquots of the cultures were harvested 20 and 60 min after glucose addition, and total RNA was extracted for all samples. For all microarray analyses, the quality of RNA was tested by using an Agilent Bioanalyzer 2100 with RNA Nano 6000 LabChips. Samples were labeled with Cy3-CTP or Cy5-CTP by using a low input fluorescent linear amplification kit (Agilent Technologies, Palo Alto, CA, USA). Labeled cRNA was purified with the RNeasy MinElute kit (Qiagen, Valencia, CA, USA) and hybridized to yeast 60-mer oligonucleotide arrays (Agilent Technologies) according to the manufacturer's instructions. Slides were scanned at 10 μm resolution with two-line averaging using an Axon GenePix 4200A scanner and GenePix 6.0 software. Ratio-based and LOWESS normalization as well as statistical analysis were done in Acuity 4.0 (Molecular Dynamics, Piscataway, NJ, USA). Misregulated genes in *gcr1*Δ were identified by an average expression change of at least twofold (i.e., a $\log_2$ ratio of ≤ -1 or ≥ 1) relative to the isogenic wild type value. Statistical significance of the genes identified by this analysis was confirmed by performing a paired, one-tailed *t*-test against a control array; genes referred to as statistically significant have a $p < 0.001$. Hierarchical clustering was done by using a centered Pearson similarity metric; *K*-means cluster analysis was done by using a Euclidean squared similarity metric. Steady-state microarrays were done in four replicate experiments, including both biological replicates and dye-swap technical replicates. Time course microarrays were done according to the method of Wang et al. (2004). *p*-values confirming the enrichment for specific MIPS functional groups were calculated as previously described (Robinson et al. 2002). All microarray data are compliant with Minimal Information About Microarray Experiments (MIAME; Brazma et al. 2001) standards, and the full datasets are available though the NCBI Gene Expression Omnibus (GEO) database (http://www.ncbi.nlm.nih.gov/projects/geo/). The accession number for steady state analysis in glucose-, galactose-, and raffinose-grown cells is GSE5027; the accession number for time course analysis is GSE5575.

Mitochondrial staining

To assay respiratory function via mitochondrial staining, isogenic cultures were grown to mid-logarithmic phase in YEP containing the indicated C-sources. Cells were first stained with MitoTracker Red CM-H_2XRos (Invitrogen, Carlsbad, CA, USA) by adding the dye to a final concentration of 225 μM and continuing incubation for 15 min. Cells were then collected by low-speed centrifugation and resuspended to a density of 1×10^7 cells/ml in 10 mM HEPES [pH 7.4] containing the indicated C-source. Cultures grown in 3% glycerol were supplemented with a low level of glucose to stimulate growth (Banuelos and Fraenkel 1982; Sherman 2002). Mitochondrial DNA was counterstained by adding SYTO 18 (Invitrogen) to a final concentration of 10 μM and incubating at room temperature for 5 min. Stained cells were then visualized on a Zeiss 510 Meta confocal laser-scanning microscope. SYTO 18 was excited by using the Argon laser set to 488 nm; resulting fluorescence was detected with a 530–600 nm band pass filter. MitoTracker Red was excited with the HeNe laser at 543 nm; resulting fluorescence was detected with a 585 nm long pass filter. Each image was captured by using a 100× Plan-Apochromat oil objective such that 1 pixel = 0.14 μm.

Results

The *gcr1*Δ growth defect is C-source independent

Cells lacking the transcriptional regulator Gcr1 fail to induce rapid growth in the presence of glucose (Willis et al. 2003). Because the glycolytic genes are well-characterized targets of Gcr1 (Clifton and Fraenkel 1981; Deminoff and Santangelo 2001; and see below), we tested growth of *gcr1*Δ cells in C-sources which require varying degrees of reliance on glycolysis for the generation of energy, ranging from almost exclusively glycolysis-dependent (glucose) to not at all (pyruvate). We included two repressing C-sources (glucose and galactose; Polakis and Bartley 1965; Lodi et al. 1991) as well as two non-repressing C-sources (raffinose and pyruvate; Stoppani 1951; Lodi et al. 1991) in this test. The *gcr1*Δ growth defect is not specific to glucose but is also detectable in galactose-, raffinose-, and pyruvate-grown cultures (Fig. 1). As expected, the doubling time of wild type cells is shortest in glucose, the preferred carbon source of all organisms; in this background, we calculated the doubling time of glucose-grown wild type cells to be 1 h, 48 min. The doubling time of wild type cells grown in the presence of either galactose or raffinose was slightly more than 4 h. The doubling time of *gcr1*Δ cells grown in glucose, galactose, or raffinose was in all cases 8 h. This is approximately four times longer than glucose-grown wild type cells, and twice as

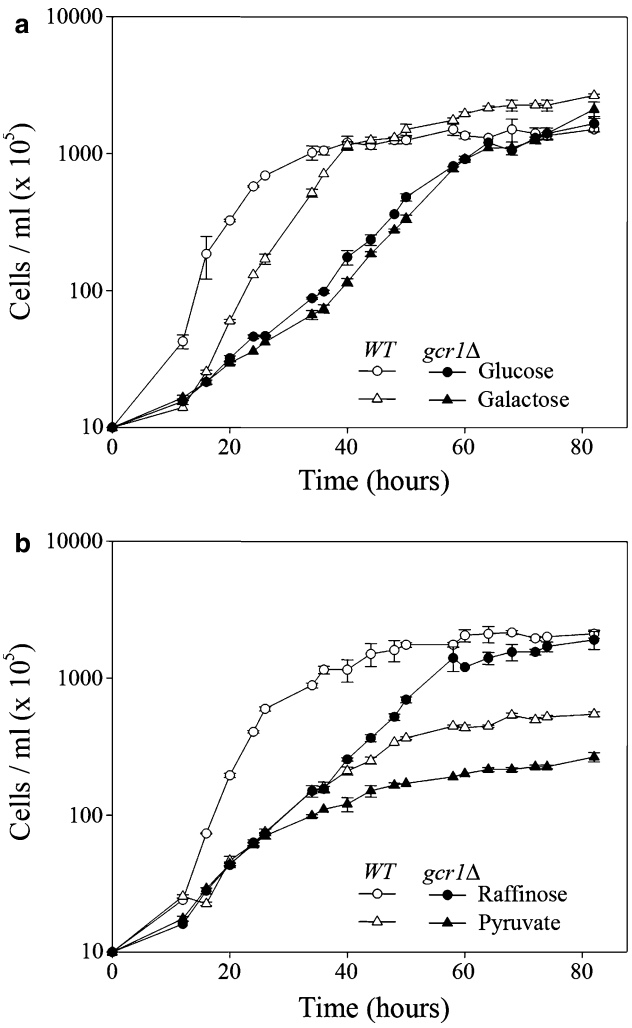

Fig. 1 Growth of *gcr1*Δ cells is impaired in all carbon sources. Isogenic strains were inoculated at a density of 1×10^6 cells/ml and incubated at 23°C to observe growth phenotypes. Wild type (*WT*; *open symbols*) and *gcr1*Δ (*closed symbols*) cells were grown in YEP containing either 2% glucose (**a**, *circles*), 3% galactose (**a**, *triangles*), 3% raffinose (**b**, *circles*) or 3% pyruvate (**b**, *triangles*). *Error bars* represent standard deviation

long as galactose- or raffinose-grown wild type cells. Despite their longer doubling times, *gcr1*Δ cultures eventually attain cell densities in stationary phase that are comparable to the corresponding wild type cultures (Fig. 1 and data not shown).

Using these values, we calculated the doubling time of wild type cells to be sixfold shorter in the presence of glucose, and threefold shorter in the presence of either galactose or raffinose, than in the presence of pyruvate. The doubling time of *gcr1*Δ cells, however, is only twofold shorter in glucose, galactose, or raffinose than the doubling time of *gcr1*Δ cells grown in pyruvate. Therefore, as previously reported for glucose (Willis et al. 2003), the addition of galactose or raffinose to the culture medium has no negative effect on growth; *gcr1*Δ cells simply lack the wild type response to added sugars and consequently exhibit no more than a modest increase in growth rate.

Genome-wide expression profiling of *gcr1*Δ cells: reduced transcription of known and novel Gcr1 targets in both repressing and derepressing C-sources

A high-throughput analysis of expression in *gcr1*Δ cells using filter hybridization technology has previously been reported (Lopez and Baker 2000). However, microarrays printed onto solid glass supports offer more efficient hybridization, greater sensitivity, and better reproducibility than filter-based arrays (Southern et al. 1999); this technical advance, in combination with improved methods for data processing and analysis (Slonim 2002), means that reliable quantitative data can now be obtained from microarray analysis. We therefore did microarray analyses to profile expression in *gcr1*Δ cells. This analysis has already been reported for pyruvate-grown cells (Santangelo 2006) and glycerol–lactate grown cells (Sasaki and Uemura 2005), so we analyzed cultures grown in glucose, galactose, and raffinose.

We identified 116 genes that exhibited a statistically significant reduction in expression in all C-sources in the absence of Gcr1 (Fig. 2a; Table 1). An analysis of the promoters of these genes shows that 86 contain a strong match to the consensus Rap1 binding site (RMACCA; Zhu and Zhang 1999) and/or interact with Rap1 in a chromatin immunoprecipitation (ChIP) assay (Lieb et al. 2001; Lee et al. 2002), while 101 have a consensus Gcr1 binding site (CWTCC; Zhu and Zhang 1999; a complete list of these genes, cross-referenced to a previously published analysis of the genome-wide location of Rap1/Gcr1 binding sites, is given in web Table S1). Not surprisingly, most of the 116 (~72% of the total) were either glycolytic or RPGs (Table 1). This result agreed with our previous identification of individual Gcr1 target genes (Deminoff and Santangelo 2001). Eleven of these genes [*FBA1*, *TPI1*, *TDH1*, *TDH2*, *TDH3*, *ENO1*, *ENO2*, *PGK1*, *GPM1*, *CDC19* (*PYK1*), and *ADH1*] were also identified as showing a twofold or greater decrease in expression in one or both of two previous large scale analyses from other labs (Lopez and Baker 2000; Sasaki and Uemura 2005). One of these studies (Sasaki and Uemura 2005) also identified 57 RPGs as having reduced expression in *gcr1*Δ cells; however, the names of the individual genes were not included in the published data, so we are unable to assess the exact degree of correlation between that study and ours.

Since asynchronous cultures were profiled we did not expect to (and in fact did not) detect the significant Gcr1-dependence of cyclin gene transcription in

glucose-grown cells (Willis et al. 2003). We did, however, identify a number of novel genes as exhibiting Gcr1-dependent transcription (Fig. 2a), including *YBR187W* [a previously uncharacterized open reading frame (ORF)] and *PET122* (which encodes a mitochondrial translation factor). The promoters of both genes contain consensus-binding sites for Rap1 and Gcr1, and Rap1 interacts with the promoter of *YBR187W* (web Table A). As previously noted (Lopez and Baker 2000), there are two ORFs, now listed as dubious, that overlap extensively with Gcr1 targets: *YKL153W*, which overlaps *GPM1*; and *YCR013C*, which overlaps *PGK1*. We have identified a third such dubious ORF, *YLL044W*, which overlaps the Gcr1 target *RPL8B*. Interestingly, these three ORFs are differentially regulated in wild type and *gcr1*Δ cells (Fig. 2a); the design of our arrays, which use single-stranded 60-mer oligonucleotide probes complementary only to the target RNA, eliminates the possibility that this difference is attributable to cross-hybridization. Recent work from several groups using high-density tiling arrays has demonstrated the existence of independent transcription units from non-coding genes in yeast (David et al. 2006; Samanta et al. 2006). The 402 naturally occurring antisense transcripts detectable in both total and poly(A) RNA samples included *YKL153W*, *YCR013C*, and *YLL044W* (David et al. 2006) suggesting the intriguing possibility that these ORFs may contribute to the regulation of *GPM1*, *PGK1*, and *RPL8B*.

K-means cluster analysis divides the 116 genes that meet the cutoff for significant reduction in *gcr1*Δ cells in all C-sources into four distinct patterns of expression (Fig. 2b). Of these 116 genes, only 20 display little or no difference in the degree to which transcript levels are reduced in glucose-, galactose-, or raffinose-grown cells (cluster I, Fig. 2b). This cluster of 20 genes displays a significant functional enrichment for genes involved in glycolysis and gluconeogenesis ($p = 3.71 \times 10^{-6}$) as well as for genes involved in amino acid biosynthesis ($p = 0.006$). Genes whose dependence on Gcr1 was equivalent in all C-sources (arrows in Fig. 2a) includes the novel targets *SUN4*, *UTR2*, *SAM1*, and *PET122*, two glycolytic genes (*CDC19* and *GPM1*), and an *RPG* (*RPS14B*). However, for most of the genes in cluster I, the ratio of *gcr1*Δ to wild type expression appears to be slightly lower in glucose-grown cells than in galactose- or raffinose-grown cells. Cluster II shows that another 25 genes have a significantly lower *gcr1*Δ to wild type ratio in galactose-grown cells than in glucose- or raffinose-grown cells; this cluster displays a significant functional enrichment for genes involved in glycolysis and gluconeogenesis ($p = 9.49 \times 10^{-6}$) as well as for genes involved in ribosome biosynthesis ($p = 1.56 \times 10^{-4}$).

For most genes affected by *GCR1* deletion, the difference in expression relative to wild type was more apparent in glucose- and galactose-grown cells than in raffinose-grown cells (71 genes total, shown in clusters III and IV, Fig. 2b). These two clusters are both significantly enriched for RPGs ($p < 1 \times 10^{-14}$). Cluster III also includes the negative regulator of translation *ASC1* and the uncharacterized essential gene *YBR187W*. Expression of *YBR187W* during the diauxic shift (DeRisi et al. 1997) and in response to glucose (Wang et al. 2004) also places it in a cluster with RPGs. Ybr187W has been shown to physically interact (Ito et al. 2001; Krogan et al. 2006) with Rpa12, Nop12, Mrd1, and Bms1, all of which participate in the synthesis and processing of rRNA (Gelperin et al. 2001; Wegierski et al. 2001; Wu et al. 2001; Jin et al. 2002; Prescott et al. 2004), as well as with Rrs1, which is a regulator of ribosome synthesis (Tsuno et al. 2000). The established method of assigning function to a gene based on its expression profile (Wu et al. 2002), and physical interactions, allow us to make the novel assignment of *YBR187W* to a role in ribosome biogenesis. We therefore give *YBR187W* the name *GDT1*, for Gcr1-Dependent Translation factor 1.

An average of the $\log_2$ ratios of all RPGs that meet the cutoff for significant down-regulation in the *gcr1*Δ mutant suggests that the defect in expression is the same within error for glucose-, galactose-, or raffinose-grown cells. However, an average for the genes in either Cluster III or IV alone shows that for a subset of RPGs, the ratio of *gcr1*Δ to wild type expression is lower in glucose- or galactose-grown cells than in raffinose-grown cells. Since it is commonly accepted that RPG expression is tightly linked to growth rate, this result is interesting and somewhat puzzling, as the doubling time of *gcr1*Δ cells grown in any of these three carbon sources is indistinguishable.

Global expression analysis of *gcr1*Δ cells shows that the misregulation of RPGs is detectable 20 min after glucose addition and is not a response to slow growth

Expression of RPGs is elaborately controlled; it is known to be coordinately regulated and linked to both cell growth and secretory function (Kief and Warner 1981; Mizuta and Warner 1994). RPGs are also subject to extensive post-transcriptional regulation and feedback control (Dabeva et al. 1986; Presutti et al. 1991; Li et al. 1995, 1996; Fewell and Woolford 1999). Furthermore, given the importance of protein synthetic capacity

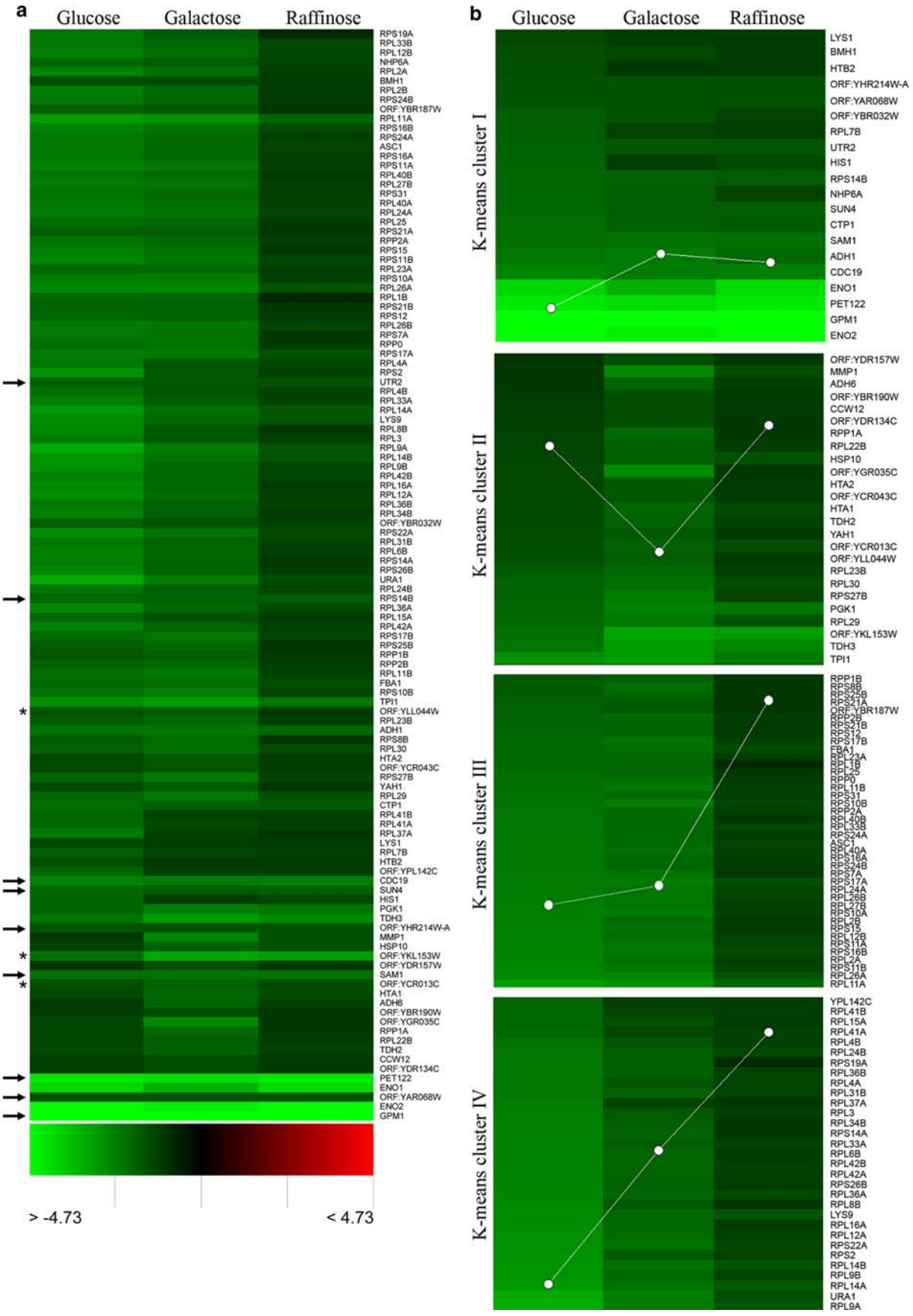
a
Glucose
Galactose
Raffinose
RPS19A
RPL33B
RPL12B
NHP6A
RPL2A
BMH1
RPL2B
RPS24B
ORF:YBR187W
RPL11A
RPS16B
RPS24A
ASC1
RPS16A
RPS11A
RPL40B
RPL27B
RPS31
RPL40A
RPL24A
RPL25
RPS21A
RPP2A
RPS15
RPS11B
RPL23A
RPS10A
RPL26A
RPL1B
RPS21B
RPS12
RPL26B
RPS7A
RPP0
RPS17A
RPL4A
RPS2
UTR2
RPL4B
RPL33A
RPL14A
LYS9
RPL8B
RPL3
RPL9A
RPL14B
RPL9B
RPL42B
RPL16A
RPL12A
RPL36B
RPL34B
ORF:YBR032W
RPS22A
RPL31B
RPL6B
RPS14A
RPS26B
URA1
RPL24B
RPS14B
RPL36A
RPL15A
RPL42A
RPS17B
RPS25B
RPP1B
RPP2B
RPL11B
FBA1
RPS10B
TPI1
ORF:YLL044W
RPL23B
ADH1
RPS8B
RPL30
HTA2
ORF:YCR043C
RPS27B
YAH1
RPL29
CTP1
RPL41B
RPL41A
RPL37A
LYS1
RPL7B
HTB2
ORF:YPL142C
CDC19
SUN4
HIS1
PGK1
TDH3
ORF:YHR214W-A
MMP1
HSP10
ORF:YKL153W
ORF:YDR157W
SAM1
ORF:YCR013C
HTA1
ADH6
ORF:YBR190W
ORF:YGR035C
RPP1A
RPL22B
TDH2
CCW12
ORF:YDR134C
PET122
ENO1
ORF:YAR068W
ENO2
GPM1
> -4.73
< 4.73
b
Glucose
Galactose
Raffinose
K-means cluster I
LYS1
BMH1
HTB2
ORF:YHR214W-A
ORF:YAR068W
ORF:YBR032W
RPL7B
UTR2
HIS1
RPS14B
NHP6A
SUN4
CTP1
SAM1
ADH1
CDC19
ENO1
PET122
GPM1
ENO2
K-means cluster II
ORF:YDR157W
MMP1
ADH6
ORF:YBR190W
CCW12
ORF:YDR134C
RPP1A
RPL22B
HSP10
ORF:YGR035C
HTA2
ORF:YCR043C
HTA1
TDH2
YAH1
ORF:YCR013C
ORF:YLL044W
RPL23B
RPL30
RPS27B
PGK1
RPL29
ORF:YKL153W
TDH3
TPI1
K-means cluster III
RPP1B
RPS8B
RPS25B
RPS21A
ORF:YBR187W
RPP2B
RPS21B
RPS12
RPS17B
FBA1
RPL23A
RPL1B
RPL25
RPP0
RPL11B
RPS31
RPS10B
RPP2A
RPL40B
RPL33B
RPS24A
ASC1
RPL40A
RPS16A
RPS24B
RPS7A
RPS17A
RPL24A
RPL26B
RPL27B
RPS10A
RPL2B
RPS15
RPL12B
RPS11A
RPS16B
RPL2A
RPS11B
RPL26A
RPL11A
K-means cluster IV
YPL142C
RPL41B
RPL15A
RPL41A
RPL4B
RPL24B
RPS19A
RPL36B
RPL4A
RPL31B
RPL37A
RPL3
RPL34B
RPS14A
RPL33A
RPL6B
RPL42B
RPL42A
RPS26B
RPL36A
RPL8B
LYS9
RPL16A
RPL12A
RPS22A
RPS2
RPL14B
RPL9B
RPL14A
URA1
RPL9A

Fig. 2 Transcriptomic analysis identifies down-regulated targets in *gcr1*Δ. Microarrays were done by competitive hybridization of RNAs from *gcr1*Δ and wild type cells grown in YEP containing either 2% glucose, 3% galactose, or 3% raffinose. **a** Hierarchical clustering was done by using a centered Pearson similarity metric on genes that exhibited at least a twofold decrease in expression in the mutant. The *scale* at the bottom shows color intensity relative to the mean $\log_2$ ratio of four replicate arrays in each carbon source. Genes whose expression was found to be equivalently defective in all C-sources, as defined by calculating ratios of the $\log_2$ expression values in glucose-, galactose-, and raffinose-grown cells and selecting for a value of 1 (±10%), are indicated by *arrows*. *Asterisks* denote dubious ORFs (see text for details). **b** *K*-means cluster analysis of the down-regulated target genes shown in **a**, generated by using a Euclidean squared similarity metric. *K*-means clusters are shown individually, with color intensity indicating the mean $\log_2$ ratio. The expression profile of the genes contained in each cluster is depicted by the overlaid line graph. *Points* on the line (*white circles*) represent the average of the $\log_2$ ratio for the genes in the cluster in either glucose-, galactose-, or raffinose-grown cells, respectively; averages are −2.4, −2.1, and −2.2 for cluster I; −1.5, −2.0, and −1.4 for cluster II; −2.2, −2.1, and −1.2 for cluster III; −2.4, −1.8, and −1.2 for cluster IV

Table 1 MIPS functional classification of differentially regulated genes in *gcr1*Δ cells grown on glucose, galactose, or raffinose

	p value
Down-regulated	
Ribosome biogenesis	1×10^{-14}
Protein synthesis	1×10^{-14}
Glycolysis/gluconeogenesis	7.54×10^{-9}
Energy	0.002
C-compound and carbohydrate utilization	0.008
Chromosome	0.008
Up-regulated	
C-compound and carbohydrate utilization	6.21×10^{-8}
C-compound and carbohydrate metabolism	5.43×10^{-7}
Stress response	4.32×10^{-6}
Pentose phosphate	5.0×10^{-4}
Energy reserves	4.8×10^{-3}
Nucleotide metabolism	6.6×10^{-3}

Genes were classified into one or more MIPS functional groups by using the web-based cluster interpreter FunSpec (Robinson et al. 2002)

for supporting the accumulation of new cell mass, it is not surprising that when the deletion of any one of the genes encoding a factor that contributes to RPG expression is viable (*GCR1*, *SFP1, FHL1*, *IFH1*, or *HMO1*), it results in a pronounced slow growth phenotype (Clifton and Fraenkel 1981; Blumberg and Silver 1991; Hermann-Le Denmat et al. 1994; Cherel and Thuriaux 1995; Lu et al. 1996). This presents a challenge for understanding the transcriptional regulation of these genes, since any effect on expression may be attributed to a variety of causes. To eliminate any metabolic or growth-related effects on expression, we examined the immediate transcriptional response of *gcr1*Δ cells to the appearance of glucose.

As a reference, we compared wild type and *gcr1*Δ cells grown in pyruvate (0 min, Fig. 3). Within 20 min of glucose addition, 41 RPGs were found to be misregulated relative to the absence of glucose (0 min vs. 20 min, Fig. 3), as identified by *K*-means clustering. Nineteen of these genes were down-regulated (asterisks in Fig. 3), while 22 were up-regulated (diamonds in Fig. 3). However, most of the observed up-regulation is transient; 60 min after glucose addition, there is reduced expression of 90 of 116 genes that are down in *gcr1*Δ cells in steady state; this includes all of the RPGs shown in Fig. 2 except *RPL41B*. This transcriptomic effect occurs before the onset of any change in growth, suggesting that the altered expression seen in this experiment is likely to be a direct result of *GCR1* deletion. RPG transcripts that remain less than twofold reduced 60 min after glucose addition are *RPS25A*, *RPS27A*, *RPS28A*, *RPS30A*, *RPS30B*, *RPL10*, *RPL41B*, *RPL15B*, and *RPP2B* (Fig. 3 and data not shown). *RPS25A*, *RPS27A*, *RPS28A*, *RPS30A*, *RPS30B*, *RPL10*, and *RPL15B* are not in the set of 116 genes identified by our previous analysis (Fig. 2a), while *RPL41B* was at the borderline of significance in galactose- and raffinose-grown cells. Transcription of *RPS28A* and *RPP2B* is known to be Rap1-independent (Mager and Planta 1991), supporting the idea that this experimental design allows us to distinguish clearly between those RPGs that are directly affected by Gcr1 and those that are influenced by coordinate regulation.

Our analysis shows that 73 of 138 total RPGs in *S. cerevisiae* exhibit a statistically significant reduction in expression in glucose-, galactose-, and raffinose-grown *gcr1*Δ cells (Fig. 2a, web Table A); for all but one of the 73, the reduction in expression is growth-rate independent (Fig. 3). Of these 72 genes, 68 have a strong Rap1 consensus-binding site and/or are known to be Rap1-bound in vivo (web Table S1). This group of 68 genes, whose reduction in expression is both growth rate-independent and statistically significant in cells grown on a non-repressing carbon source, represents our high-confidence dataset for RPGs that are affected by Gcr1.

The large size (*lge*) phenotype of *gcr1*Δ cells is specific to growth on a repressing sugar

Yeast mutants defective in either protein biosynthesis or carbon metabolism have been shown to exhibit cell size phenotypes (Jorgensen et al. 2002). Glucose-grown *gcr1*Δ cells are known to exhibit a *lge* phenotype; this phenotype is linked to both low levels of *CLN* mRNA and a severely reduced protein synthetic rate (Willis et al. 2003). We show here that expression

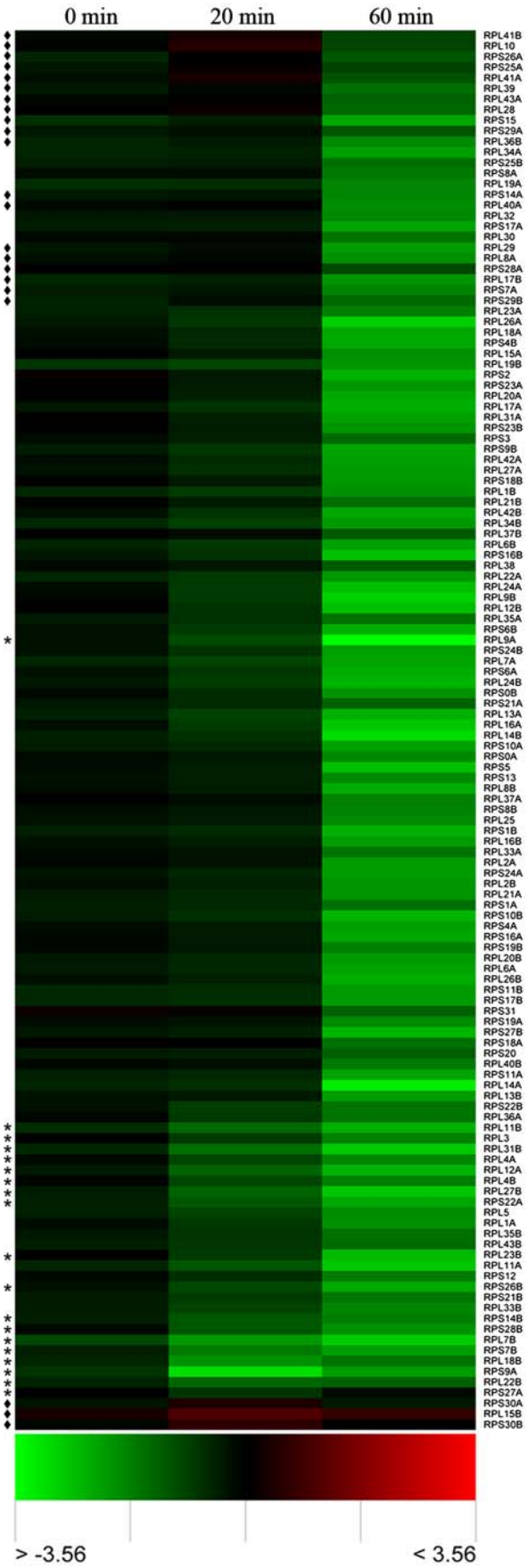

◀ **Fig. 3** The *gcr1*Δ defect in expression of RPGs can be detected as early as 20 min after carbon source up-shift. Time course microarrays were done by competitive hybridization of RNAs from *gcr1*Δ and wild type cells grown in YEP in the absence of glucose (0 min) or after glucose addition (20 and 60 min). The *scale* at the bottom shows color intensity relative to the $\log_2$ ratio of expression in *gcr1*Δ and wild type cells. Genes whose expression exhibits a decrease (indicated by *asterisks*) or an increase (indicated by *diamonds*) relative to wild type 20 min after glucose addition were identified by *K*-means cluster analysis (data not shown)

of some Gcr1-dependent RPGs varies in a C-source dependent manner (Fig. 2b), suggesting the possibility that in *gcr1*Δ cells, protein biosynthetic rates and/or cell cycle progression may also vary with C-source. If this is the case, then *gcr1*Δ cell size might also be expected to vary, since the doubling time of *gcr1*Δ cells remains the same in all C-sources. We therefore measured the size of *gcr1*Δ cells in different C-sources to test whether the *lge* phenotype was C-source independent or instead might vary in a C-source dependent manner. We first measured wild type cells, which are known to undergo a slight increase in cell size during rapid growth on glucose (Johnston et al. 1979; Tokiwa et al. 1994). This was indeed observed as a modest shift of the cell volume peak for glucose compared to cells grown in other C-sources (Fig. 4a). The *lge* phenotype of *gcr1*Δ cells, which is pronounced in glucose, is at least as severe in galactose (Fig. 4b). Significantly, there was no detectable cell size phenotype during growth on the non-repressing C-sources raffinose and pyruvate (Fig. 4b). To confirm that this effect is specific to Gcr1 removal we measured *cln3*Δ cells, which are defective in G1 progression and well-characterized as having a *lge* phenotype in glucose (Nash et al. 1988). Importantly, unlike *gcr1*Δ cells, *cln3*Δ cells are larger to approximately the same extent in each of the C-sources tested (Fig. 4c).

Gcr1 removal results in both a genome-wide defect in glucose repression and an increase in the expression of stress response genes

Our microarray analysis also identified 118 genes whose transcription exhibited a statistically significant increase in glucose-, galactose-, and raffinose-grown *gcr1*Δ cells (Fig. 5a). Only 28 of these genes either contain a consensus Rap1 site in their promoter (Zhu and Zhang 1999) and/or are bound by Rap1 (Lieb et al. 2001; Lee et al. 2002), although 97 contain a consensus Gcr1 binding site (Zhu and Zhang 1999; a complete list of these genes is given in web Table S2). The motif discovery algorithm MEME (Bailey et al. 2006) did not identify any other sequence elements common to the

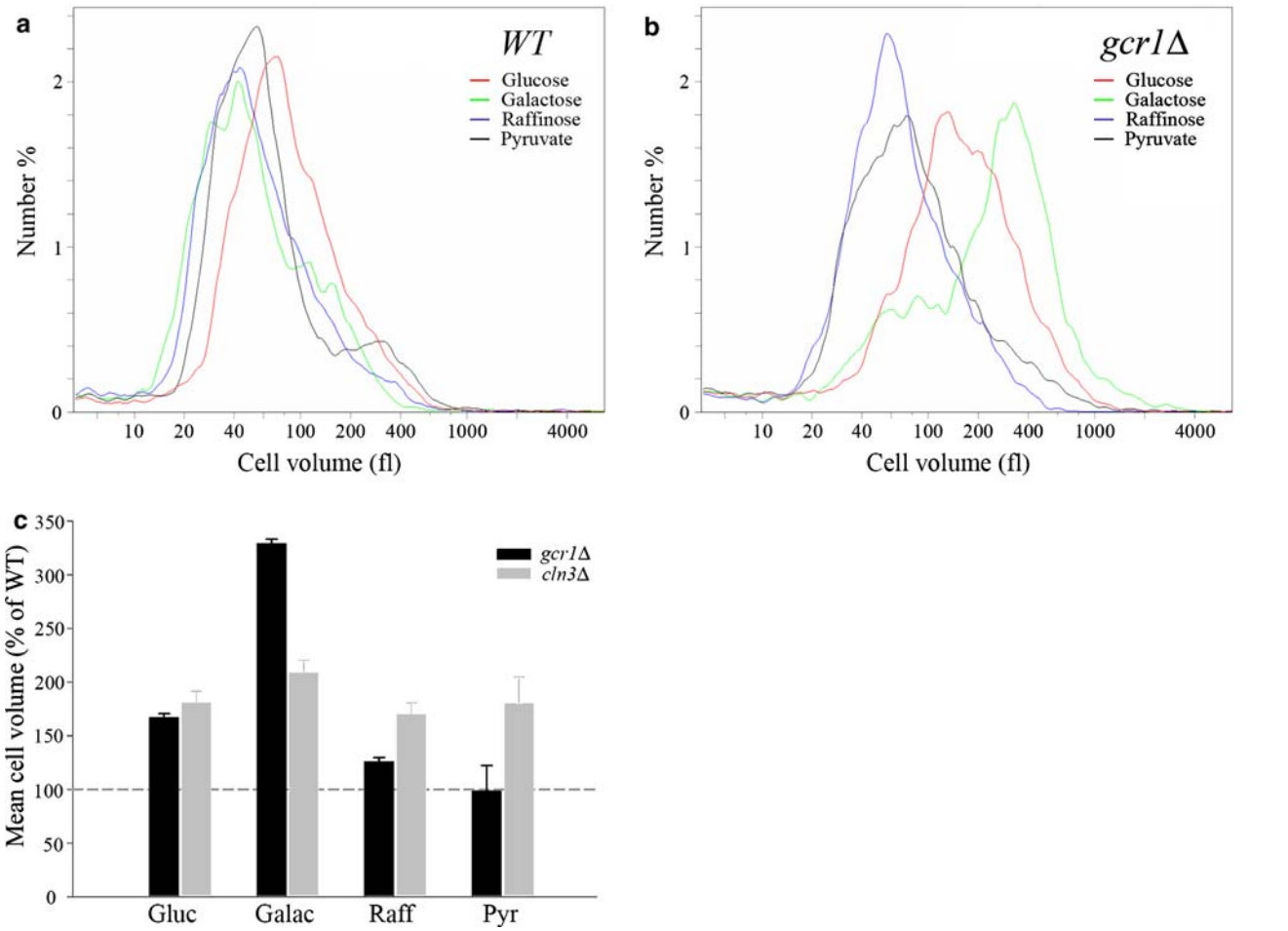

Fig. 4 *gcr1*Δ cells have a carbon source dependent large size phenotype. Cell size distributions from wild type (*WT*, **a**) and *gcr1*Δ cells (**b**) growing in YEP containing 2% glucose, 3% galactose, 3% raffinose, or 3% pyruvate as the carbon source were collected during mid-logarithmic phase. Cell volume (fl) is plotted relative to number percent of the population. Each determination represents ~10,000 cells. **c** The mean cell volume from *gcr1*Δ and *cln3*Δ cells is plotted as a percentage of the corresponding wild type value for each of the four carbon sources. Each *bar* represents the average of duplicate samples collected at three time points during mid-logarithmic growth. *Error bars* denote standard deviation and a *dashed line* representing the wild type value (set to 100%) is included for reference

promoters of all 118 genes. Since a CT box alone is insufficient for Gcr1 to function in vivo (Buchman et al. 1988; Zeng et al. 1997), the influence of *GCR1* deletion on some of these genes may occur as a result of changes in highly networked regulatory pathways. Notable exceptions whose promoters contain both a Rap1 site and a consensus CT box are the transcription factor *TYE7*, the stationary-phase induced gene *SNZ1*, the glucose-regulated stress response factor *HSP12*, the transketolase *TKL2*, and the inosine monophosphate dehydrogenase *IMD2*, which catalyzes the first step of GMP biosynthesis.

Multiple processes that are normally either silent or weakly expressed in glucose- or galactose-grown cells (Table 1), including alternative C-compound metabolism and the pentose phosphate pathway, were significantly enriched among the genes in this dataset. This was not surprising, since Gcr1 is known to participate in glucose repression (Turkel et al. 2003; Sasaki and Uemura 2005), and five of these genes (*GLK1*, *DLD3*, *CIT1*, *CIT3*, and *CIT2*) were previously identified as having significantly increased expression in *gcr1*Δ cells (Sasaki and Uemura 2005). Additionally, there was a significant enrichment in this dataset for genes that are functionally annotated to the stress response (*YRO2*, *GRX3*, *HSP78*, *HSP12*, *DAK2*, *CTT1*, *DAK1*, *SNO1*, *SNZ1*, *PAI3*, *YGP1*, *DDR2*, *YOR054C*, and *ATH1*). However, more than half of these 14 genes are also upregulated in response to the diauxic shift (DeRisi et al. 1997). It has recently been suggested that activation of some component of the stress response may be required for the switch between fermentative and

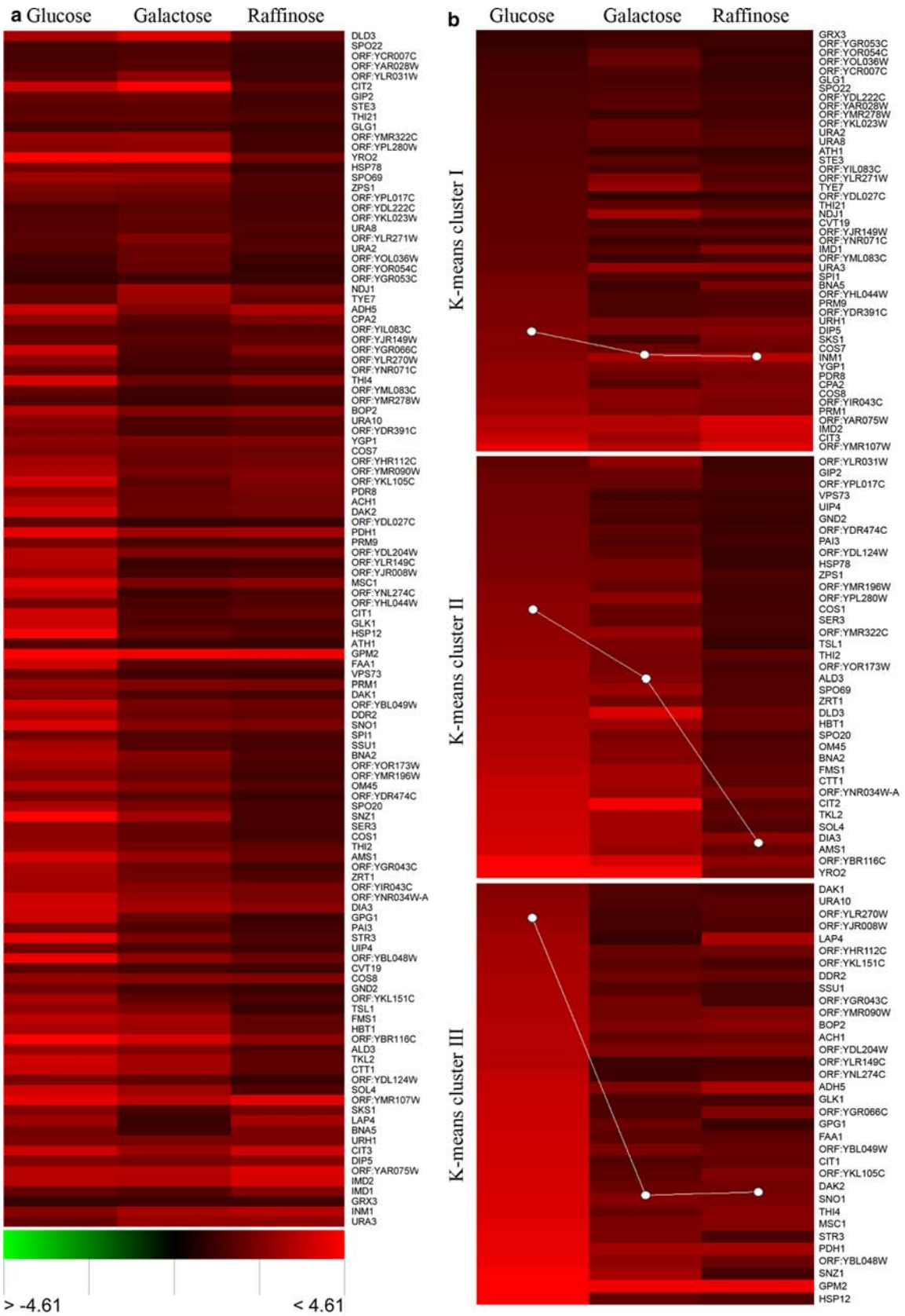
a Glucose
Galactose
Raffinose
DLD3
SPO22
ORF:YCR007C
ORF:YAR028W
ORF:YLR031W
CIT2
GIP2
STE3
THI21
GLG1
ORF:YMR322C
ORF:YPL280W
YRO2
HSP78
SPO69
ZPS1
ORF:YPL017C
ORF:YDL222C
ORF:YKL023W
URA8
ORF:YLR271W
URA2
ORF:YOL036W
ORF:YOR054C
ORF:YGR053C
NDJ1
TYE7
ADH5
CPA2
ORF:YIL083C
ORF:YJR149W
ORF:YGR066C
ORF:YLR270W
ORF:YNR071C
THI4
ORF:YML083C
ORF:YMR278W
BOP2
URA10
ORF:YDR391C
YGP1
COS7
ORF:YHR112C
ORF:YMR090W
ORF:YKL105C
PDR8
ACH1
DAK2
ORF:YDL027C
PDH1
PRM9
ORF:YDL204W
ORF:YLR149C
ORF:YJR008W
MSC1
ORF:YNL274C
ORF:YHL044W
CIT1
GLK1
HSP12
ATH1
GPM2
FAA1
VPS73
PRM1
DAK1
ORF:YBL049W
DDR2
SNO1
SPI1
SSU1
BNA2
ORF:YOR173W
ORF:YMR196W
OM45
ORF:YDR474C
SPO20
SNZ1
SER3
COS1
THI2
AMS1
ORF:YGR043C
ZRT1
ORF:YIR043C
ORF:YNR034W-A
DIA3
GPG1
PAI3
STR3
UIP4
ORF:YBL048W
CVT19
COS8
GND2
ORF:YKL151C
TSL1
FMS1
HBT1
ORF:YBR116C
ALD3
TKL2
CTT1
ORF:YDL124W
SOL4
ORF:YMR107W
SKS1
LAP4
BNA5
URH1
CIT3
DIP5
ORF:YAR075W
IMD2
IMD1
GRX3
INM1
URA3
> -4.61
< 4.61
b
Glucose
Galactose
Raffinose
K-means cluster I
GRX3
ORF:YGR053C
ORF:YOR054C
ORF:YOL036W
ORF:YCR007C
GLG1
SPO22
ORF:YDL222C
ORF:YAR028W
ORF:YMR278W
ORF:YKL023W
URA2
URA8
ATH1
STE3
ORF:YIL083C
ORF:YLR271W
TYE7
ORF:YDL027C
THI21
NDJ1
CVT19
ORF:YJR149W
ORF:YNR071C
IMD1
ORF:YML083C
URA3
SPI1
BNA5
ORF:YHL044W
PRM9
ORF:YDR391C
URH1
DIP5
SKS1
COS7
INM1
YGP1
PDR8
CPA2
COS8
ORF:YIR043C
PRM1
ORF:YAR075W
IMD2
CIT3
ORF:YMR107W
K-means cluster II
ORF:YLR031W
GIP2
ORF:YPL017C
VPS73
UIP4
GND2
ORF:YDR474C
PAI3
ORF:YDL124W
HSP78
ZPS1
ORF:YMR196W
ORF:YPL280W
COS1
SER3
ORF:YMR322C
TSL1
THI2
ORF:YOR173W
ALD3
SPO69
ZRT1
DLD3
HBT1
SPO20
OM45
BNA2
FMS1
CTT1
ORF:YNR034W-A
CIT2
TKL2
SOL4
DIA3
AMS1
ORF:YBR116C
YRO2
K-means cluster III
DAK1
URA10
ORF:YLR270W
ORF:YJR008W
LAP4
ORF:YHR112C
ORF:YKL151C
DDR2
SSU1
ORF:YGR043C
ORF:YMR090W
BOP2
ACH1
ORF:YDL204W
ORF:YLR149C
ORF:YNL274C
ADH5
GLK1
ORF:YGR066C
GPG1
FAA1
ORF:YBL049W
CIT1
ORF:YKL105C
DAK2
SNO1
THI4
MSC1
STR3
PDH1
ORF:YBL048W
SNZ1
GPM2
HSP12

Fig. 5 Transcriptome analysis identifies up-regulated targets in *gcr1*Δ. Microarrays were done by competitive hybridization of RNAs from *gcr1*Δ and wild type cells grown in YEP containing either 2% glucose, 3% galactose, or 3% raffinose. **a** Hierarchical clustering was done on genes that exhibited at least a twofold increase in expression in the mutant by using a centered Pearson similarity metric. The *scale* at the bottom shows color intensity relative to the mean $\log_2$ ratio of four replicate arrays. **b** *K*-means cluster analysis of the up-regulated target genes shown in **a**, generated by using a Euclidean squared similarity metric. *K*-means clusters are shown individually, with color intensity indicating the mean $\log_2$ ratio. The expression profile of the genes contained in each cluster is depicted by the overlaid line graph. *Points* on the line (*white circles*) represent the average of the $\log_2$ ratio for the genes in the cluster in glucose-, galactose-, or raffinose-grown cells, respectively; averages are 2.0, 1.9, and 1.9 for cluster I; 2.9, 2.5, and 1.5 for cluster II; 3.6, 1.9, and 2.0 for cluster III

oxidative metabolism (Brauer et al. 2005). Since *gcr1*Δ cells display no significant increase in thermotolerance (data not shown), it seems likely that the enrichment for stress response genes is linked to changes in carbon metabolism (see below).

Using *K*-means cluster analysis, we divided the 118 genes that exhibit a significant increase in expression into three groups. Slightly less than half (47 genes, shown in cluster I, Fig. 5b) show little or no difference in expression between glucose-, galactose-, or raffinose-grown cells. This cluster is functionally enriched for genes involved in nucleotide metabolism ($p = 1.01 \times 10^{-4}$), and specifically for genes involved in ribonucleotide metabolism.

Genes in clusters II and III have a significantly higher *gcr1*Δ to wild type ratio in glucose-grown cells than in galactose- or raffinose-grown cells; these clusters display a significant functional enrichment for genes involved in C-compound metabolism ($p = 5.27 \times 10^{-4}$) and C-compound and carbohydrate utilization ($p = 6.89 \times 10^{-6}$), respectively. Additionally, cluster II is functionally enriched for genes that are part of the pentose-phosphate pathway ($p = 1.19 \times 10^{-3}$). These results are strongly suggestive of a genome-wide alteration in carbon metabolism in *gcr1*Δ cells.

Comparison of glucose signaling in wild type and *gcr1*Δ cells

To place the effect of *GCR1* deletion on the cells' transcriptional program into a larger biological context, we compared our microarray data to a previously published analysis of the glucose response in wild type cells (Wang et al. 2004). There is a strong inverse correlation in the expression of nutrient responsive genes in wild type and *gcr1*Δ cells upon the appearance of glucose. Twenty minutes after glucose addition, transcription of 1,651 (1,067 + 584) genes is repressed at least twofold by wild type cells. Of these 1,651 genes, 584, or 35%, show a twofold or greater increase in transcription in *gcr1*Δ cells over the same interval of time (Fig. 6a); in contrast, only 131, or 8%, decrease (data not shown).

The intersection between the set of genes that is repressed in wild type cells and the set of genes that is up-regulated in *gcr1*Δ cells is most significantly enriched for genes involved in energy metabolism, C-compound and carbohydrate utilization, respiration, C-compound and carbohydrate metabolism, and the TCA cycle (Table 2), consistent with a relief from glucose repression in *gcr1*Δ cells. Other functional categories enriched in the intersection include stress response genes and genes that participate in amino acid catabolism. Genes involved in amino acid metabolism and biosynthesis are also significantly enriched among the 996 genes up-regulated in *gcr1*Δ cells in response to glucose (Fig. 6a; Table 2); this is intriguing in light of a recent bioinformatics-based study that suggested Gcr1 may act downstream of Cha4 (MacIsaac et al. 2006), a zinc-finger transcription factor required for the catabolism of serine and threonine (Holmberg and Schjerling 1996).

The inverse correlation described above also holds true for genes that increase in wild type relative to those that decrease in the *gcr1*Δ mutant 20 min after the appearance of glucose. About 1,103 (727 + 376) genes are induced twofold or more in wild type cells in

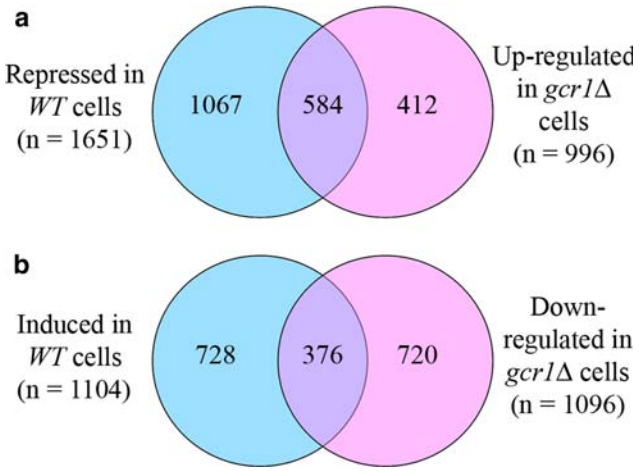

Fig. 6 A comparison of the glucose response in wild type and *gcr1*Δ cells. **a** and **b** Venn diagrams showing a comparison between the transcriptomic response of *gcr1*Δ to glucose and the previously reported (Wang et al. 2004) wild type response to glucose. Thirty-five percent of the genes that are repressed in wild type cells in response to glucose are expressed at a higher level in *gcr1*Δ cells (**a**) and 34% of the genes that are induced in wild type cells are expressed at a lower level in *gcr1*Δ cells (**b**)

Table 2 Comparison of glucose repressed genes in wild type cells with glucose induced genes in *gcr1*Δ cells

MIPS functional classification of 584 overlapping genes[a]	*p* value
Energy	$<1 \times 10^{-14}$
C-compound and carbohydrate utilization	$<1 \times 10^{-14}$
Mitochondrion	$<1 \times 10^{-14}$
Respiration	1.01×10^{-14}
C-compound and carbohydrate metabolism	2.11×10^{-13}
Tricarboxylic-acid pathway	1.29×10^{-12}
Glycolysis and gluconeogenesis	1.61×10^{-7}
Peroxisome	8.76×10^{-7}
Mitochondrial transport	8.27×10^{-6}
Stress response	2.32×10^{-5}
Glyoxylate cycle	3.83×10^{-5}
Amino acid degradation	4.29×10^{-5}
Proteolytic degradation	5.61×10^{-5}
Fermentation	1.20×10^{-4}
Oxidation of fatty acids	1.24×10^{-4}
Homeostasis of protons	2.18×10^{-4}
Pentose-phosphate pathway	6.33×10^{-4}
Lysosomal and vacuolar degradation	0.00109
Transport ATPases	0.00184
Other energy generation activities	0.00226
Lipid, fatty-acid, and isoprenoid utilization	0.00803
Cytoskeleton	0.00940
MIPS functional classification of 1,067 non-overlapping genes repressed in wild type[b]	***p* value**
Unclassified proteins	1.25×10^{-14}
Metabolism of energy reserves	9.36×10^{-11}
Proteolytic degradation	1.69×10^{-9}
Peroxisomal transport	5.21×10^{-5}
Lipid transporters	0.00206
Cytoplasmic and nuclear degradation	0.00338
ABC transporters	0.00922
MIPS functional classification of 412 non-overlapping genes induced in *gcr1*Δ[b]	***p* value**
Amino acid metabolism	1.68×10^{-13}
Amino acid biosynthesis	1.79×10^{-12}
Cation transporters	2.93×10^{-5}
Ion transporters	3.56×10^{-5}
Amino acid transport	4.91×10^{-4}
Other cation transporters (Na, K, Ca, NH_4, etc.)	6.18×10^{-4}
Nitrogen and sulfur utilization	6.18×10^{-4}
Transport facilitation	0.00115
Nitrogen and sulfur metabolism	0.00121
Homeostasis of protons	0.00159
Ionic homeostasis	0.00343
Homeostasis of cations	0.00358
Stress response	0.00508
Detoxification	0.00653
Transport ATPases	0.00711

Wild type glucose response reference data is from the 20 and 0 min exposure to glucose microarrays in Wang et al. (2004)

[a] Overlapping gene groups from Fig. 6b

[b] Non-overlapping gene groups from Fig. 6b

response to glucose, 34% of which are down-regulated twofold or more in *gcr1*Δ cells. However, only 75, or 7%, are induced in *gcr1*Δ cells (data not shown). The 376 genes that represent the intersection between these two sets function almost exclusively in rRNA and tRNA biosynthesis (Fig. 6b; Table 3); these RNA components of the translational machinery are necessary to support maximum cell growth. Glucose addition induces a further set of rRNA and tRNA genes in wild type cells (Table 3). Interestingly, cell cycle genes are among those whose expression is decreased in the *gcr1*Δ mutant in response to glucose (Table 3), consistent

Table 3 Comparison of glucose induced genes in wild type cells with glucose repressed genes in *gcr1*Δ cells

MIPS functional classification of 376 overlapping genes[a]	*p* value
rRNA transcription	$<1 \times 10^{-14}$
rRNA synthesis	2.18×10^{-10}
tRNA transcription	5.47×10^{-8}
rRNA processing	5.57×10^{-7}
tRNA modification	4.01×10^{-6}
Transcription	8.86×10^{-6}
tRNA synthesis	4.89×10^{-5}
MIPS functional classification of 728 non-overlapping genes induced in wild type[b]	***p* value**
rRNA processing	$<1 \times 10^{-14}$
rRNA transcription	$<1 \times 10^{-14}$
Transcription	3.44×10^{-9}
Translation	2.04×10^{-5}
Aminoacyl-tRNA-synthetases	6.39×10^{-4}
Pyrimidine ribonucleotide metabolism	0.00105
Nucleotide metabolism	0.00144
rRNA synthesis	0.00373
tRNA transcription	0.00594
Amino acid biosynthesis	0.00810
RNA transport	0.00935
MIPS functional classification of 720 non-overlapping genes repressed in *gcr1*Δ[b]	***p* value**
Cell cycle	1.67×10^{-5}
Cell cycle and DNA processing	2.31×10^{-5}
Mitotic cell cycle and cell cycle control	3.02×10^{-4}
Cell differentiation	3.40×10^{-4}
Fungal cell differentiation	3.40×10^{-4}
Pheromone response, mating-type determination, sex-specific proteins	0.00109
Cell fate	0.00168
Unclassified proteins	0.00369

Wild type glucose response reference data is from the 20 and 0 min exposure to glucose microarrays in Wang et al. (2004)

[a] Overlapping gene groups from Fig. 6a

[b] Non-overlapping gene groups from Fig. 6a

with an imbalance in growth and cell cycle progression (Willis et al. 2003).

Mitochondrial staining reveals that *gcr1*Δ cells respire in the presence of repressing sugars

Since *gcr1*Δ cells are defective in repression of numerous genes that encode mitochondrial functions, we used a respiration-dependent mitochondrial stain, MitoTracker Red CM-H_2XRos, to confirm that mitochondrial function is derepressed in the absence of Gcr1. The MitoTracker probe is added to cells in its reduced form and is not fluorescent unless it enters an actively respiring cell. In respiring cells the probe is oxidized to its fluorescent form and is sequestered in the mitochondria. To confirm its specificity we co-localized the MitoTracker signal with a fluorescent mitochondrial DNA stain (SYTO 18). When the media is supplemented with either glucose or galactose, mitochondria in *gcr1*Δ cells are active despite the presence of a repressing sugar; this is in stark contrast to the inactive mitochondria of wild type cells (Polakis and Bartley 1965; Fig. 7; Table 4). Mitochondrial activity in vivo therefore correlates with the genome-wide glucose repression defect that was observed with expression profiling. Further, quantitation of MitoTracker staining (Table 4) demonstrated that the percentage of respiring *gcr1*Δ cells grown on repressing sugars is as large as the percentage of respiring wild type cells grown on non-repressing C-sources (pyruvate and glycerol).

Discussion

The global regulator Gcr1 activates transcription of three classes of gene products that influence the transition through Start in the G1 phase of the cell cycle: glycolytic enzymes, ribosomal proteins, and cyclins (Clifton and Fraenkel 1981; Santangelo and Tornow 1990; Tornow et al. 1993; Zeng et al. 1997; Deminoff

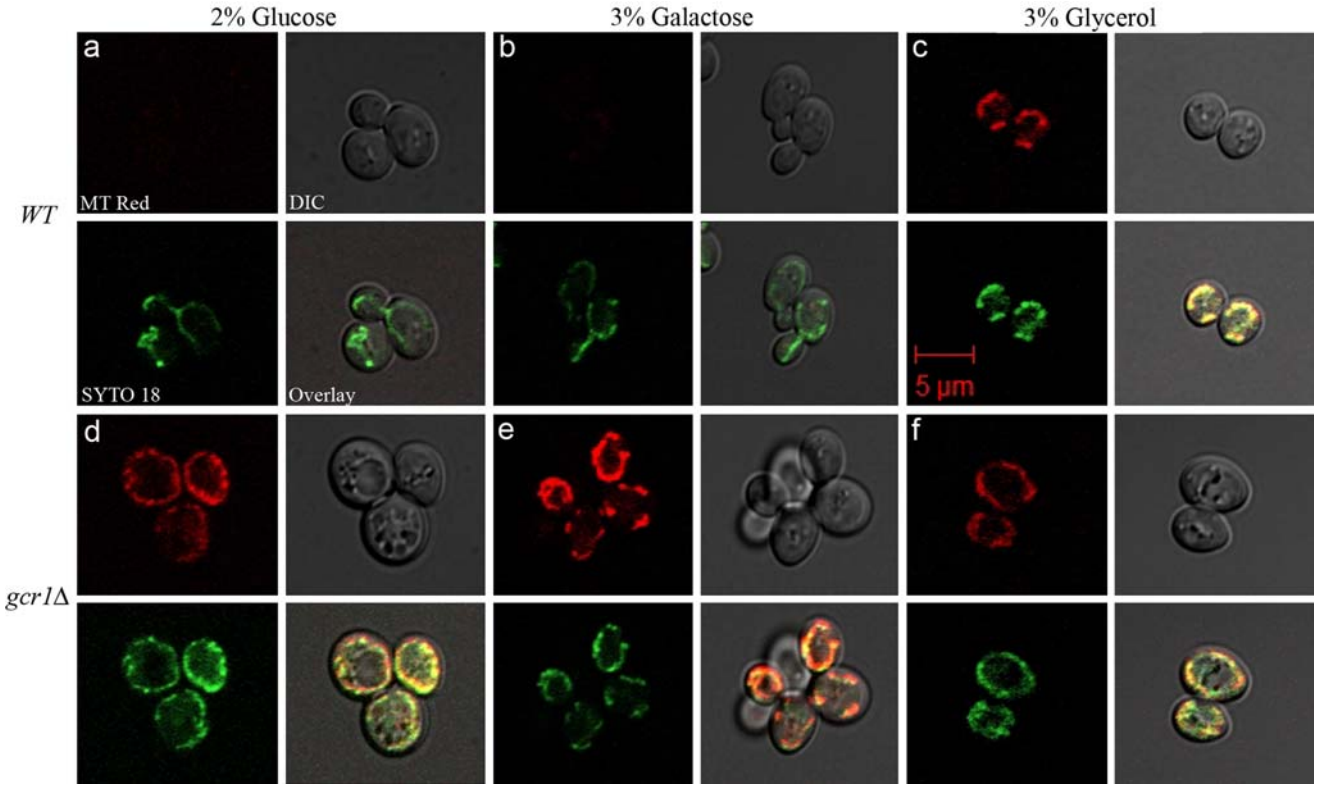

Fig. 7 *gcr1*Δ cells respire in repressing C-sources. Wild type (*WT*) and *gcr1*Δ cells were grown in YEP containing either 2% glucose (**a** and **d**), 3% galactose (**b** and **e**), or 3% glycerol (**c** and **f**) as the carbon source. Each panel shows mid-logarithmic cells stained with the respiration-dependent fluorescent dye, MitoTracker Red CM-H_2XRos (*MT Red*; *top left quadrant* of each panel) and counterstained with the mitochondrial DNA fluorescent dye, SYTO 18 (*bottom left quadrant*). The corresponding DIC image is shown in the *top right quadrant*. The *bottom right quadrant* shows all three of these quadrants merged into one image. Quantitation of MT Red staining for each condition is shown in Table 4. Though as expected pyruvate-grown cells have active mitochondria that can be detected in this assay (see Table 4), glycerol-grown cells are shown as the positive control because for unknown reasons they stain more brightly with MitoTracker

Table 4 Respiration-dependent mitochondrial staining of *gcr1*Δ cells

Growth medium	Percentage of cells stained[a,b]	
	WT	*gcr1*Δ
YEP + 2% glucose	<5[c]	78.2 ± 10.1
YEP + 3% galactose	<5[c]	83.2 ± 9.3
YEP + 3% glycerol	88.1 ± 4.7	83.9 ± 6.0
YEP + 3% pyruvate	89.8 ± 7.1	92.5 ± 5.0

[a] Cells were counted as stained with the respiration-dependent MitoTracker probe if observed fluorescence overlapped with mitochondrial DNA stained with SYTO 18

[b] Error denotes standard deviation; percentages were determined from ~450 to 500 cells for each condition

[c] Not detectable above background

and Santangelo 2001; Willis et al. 2003); transcription of these genes makes up more than 75% of pol II transcripts in rapidly growing cells (Santangelo and Tornow 1990; Warner 1999). The *gcr1*Δ mutant, which is known to be defective in exiting G1 (Willis et al. 2003), divides at a slow rate regardless of the catabolic pathways employed or the richness of the energy source (repressing and non-repressing, as well as fermentable and non-fermentable, C-sources were tested; Fig. 1).

In the absence of Gcr1, transcription of two glycolytic genes—*CDC19* and *GPM1*—was equally defective irrespective of the C-source (arrows in Fig. 2a). Since the product of *CDC19* (which encodes pyruvate kinase) does not participate in gluconeogenesis, its reduced expression in pyruvate-grown *gcr1*Δ cells (Zeng et al. 1997; Santangelo 2006) likely makes no contribution to the corresponding growth defect. It is certainly possible that one or more of the remaining six genes that exhibit unconditionally altered expression in the absence of Gcr1 (*RPS14B*, *GPM1*, *SAM1*, *PET122*, *SUN4*, and *UTR2*) account entirely for the C-source independent *gcr1*Δ growth defect. However we favor an alternative explanation—that the failure to properly regulate expression of the remaining 227 Gcr1-dependent genes is at least partly responsible for the inability

of *gcr1*Δ cells to muster more than a meager increase in the rate of cell division in the presence of even the richest source of energy, glucose. If this idea is correct, Gcr1 is one of but a few master regulators of growth/cell cycle coordination (see below).

We show here that slightly more than half of all RPGs are affected by *GCR1* deletion when cells are grown in either a repressing or a non-repressing C-source (Fig. 2). We also show that reduced expression of RPGs in *gcr1*Δ cells grown in the repressing C-source glucose cannot be attributed either to slow growth or secondary metabolic effects (Fig. 3). This is consistent with earlier work showing that abolition of Gcr1 dimerization results defects in RPG expression without resulting in a slow growth phenotype (Deminoff and Santangelo 2001). However, it is in conflict with the previously published filter hybridization-based genome-wide analysis of expression in *gcr1*Δ cells (Lopez and Baker 2000), which reports an increase in RPGs expression in glycerol–lactate grown cells. We do not observe an increase in RPG expression in *gcr1*Δ cells during steady-state growth on a non-repressing C-source, as measured on either a global level [(raffinose-grown cells; (Fig. 2) or pyruvate-grown cells; (Santangelo 2006) and time zero in (Fig. 3)], or on the level of the individual gene (S1 and primer extension analysis of RPG expression in either pyruvate-grown or glycerol–lactate grown cells; our unpublished data). This discrepancy may be attributable to the different platforms used in this and the earlier study.

Based upon the above conclusions as well as our previously published work, most if not all of the glycolytic and translational component genes identified in this study are likely to be directly stimulated targets of Gcr1. However, it is important to confirm that altered transcription of a gene identified with expression profiling reflects direct targeting by a given regulator, rather than a complex readout generated by a cross-talking network of transcription factors. This requires at minimum that the regulator in question be shown to interact with the putative target gene. Genome-wide location data (Lee et al. 2002) are available for all 141 transcription factors listed in the Yeast Protein Database (Costanzo et al. 2000), including Gcr1 and the other components of its activation assemblage (Rap1 and Gcr2; Deminoff and Santangelo 2001; Santangelo 2006). Genes identified in our profiling experiments for which location analysis provides confirmation of direct targeting by Gcr1 are *TPI1*, *ADH1*, *CDC19*, *GPM1*, *TDH3*, *RPL1B*, and *RPS19A* (Lee et al. 2002). However, at least where Gcr1 is concerned there must be numerous false negatives in the genome-wide location analysis; for example, genomic foot printing has confirmed that Gcr1 binds in vivo to *ENO1*, *ENO2*, and *PGK1* (Henry et al. 1994). Though similar confirmation has been difficult to obtain for individual *RPG*s via ChIP with epitope-tagged Gcr1 (data not shown), it seems unlikely that *RPL1B* and *RPS19A* will prove the only *bona fide* direct *RPG* targets of the Gcr1 regulator.

With respect to its involvement in glucose repression, direct interaction between Gcr1 and the canonical glucose-repressed gene *SUC2* has been established (Turkel et al. 2003; and our unpublished data). However, though we have shown that Gcr1 is required for glucose repression of mitochondrial gene function (Fig. 7), neither *SUC2* nor the glucose-repressed genes detected here (Fig. 5) were identified as direct targets via genome-wide location analysis (Lee et al. 2002). In combination with the aforementioned result for putative *RPG* targets of Gcr1, continued acceptance of the recruitment paradigm of gene regulation leaves us with an uncomfortable choice regarding these data. Either the interaction between Gcr1 and most of its direct targets is too subtle to detect with the ChIP technique, or Gcr1 influences some glycolytic genes, *RPG*s, and glucose-repressed genes directly, and other genes within these same classes indirectly. What makes this even more puzzling is that most of the promoters in question have an identical profile of specific DNA binding sites (e.g., Rap1 sites in RPG promoters).

The reverse recruitment paradigm of gene regulation (Santangelo 2006) may allow us to resolve this conundrum. Gcr1 involvement in both activation (Menon et al. 2005) and repression (our unpublished data) occurs via a reverse recruitment mechanism. If target genes are attracted to a megalithic protein assemblage while active, and are released from this assemblage when inactive, whether or not a given interaction between a regulator and its putative target gene can be detected will almost certainly be subject to spurious influences. For example, a false negative may be obtained because the position of a subunit within the assemblage places it many subunits away from the DNA helix and therefore (at least in a standard ChIP assay) incapable of pulling *bona fide* target genes into an immunoprecipitated pellet. Clearly much work remains in characterizing the physical relationships between Gcr1, its regulatory partners and targeted chromatin. Indeed, the reverse recruitment idea postulates that nuclear suprastructure is a central feature of many (if not all) gene regulatory mechanisms.

While investigating the effects of C-source on *gcr1*Δ cells we also discovered two new aspects of the *gcr1*Δ phenotype. First, *gcr1*Δ cells respire in the presence of fermentable sugars; whether this altered lifestyle is a

cause or effect of the changes we observe in glucose-regulated gene expression is a very interesting question. Changes in gene expression may cause mitochondria to become active. One model that fits into this category is that Rap1 and Gcr1 directly affect the expression of one or more genes, such as *PET122*, *SNZ1*, and/or *HSP12* that trigger the shift from fermentative to non-fermentative metabolism. According to this model, deletion of *gcr1*Δ causes the switch to be flipped inappropriately, resulting in actively respiring mitochondria in glucose-grown cells. Another model is that actively respiring mitochondria are the result of reduced glycolytic flux, brought about by reduced expression of glycolytic genes in the mutant. Alternatively, actively respiring mitochondria may signal for changes in gene expression. One possibility that fits into this category is that the cell senses changes in the GDP/GTP ratio, as the tricarboxylic acid cycle produces GTP; interestingly, expression of genes required for ribonucleotide biosynthesis are increased in *gcr1*Δ cells.

The second new feature of the *gcr1*Δ phenotype reported here is that the large cell size of the mutant is dependent upon the presence of a repressing sugar. This is also true of cells lacking Sfp1, another activator of *RPG* expression (Jorgensen et al. 2002). However, *sfp1*Δ cells exhibit the exact opposite response, i.e., in the presence of a repressing sugar *gcr1*Δ cells are larger whereas *sfp1*Δ cells are smaller (Jorgensen et al. 2004; Cipollina et al. 2005). There are two different models, which are not mutually exclusive, that may resolve this apparent paradox. The first model postulates that Gcr1 and Sfp1 have qualitatively different effects on protein biosynthesis, resulting in opposite effects on cell size. Consistent with this idea, *sfp1*Δ and *gcr1*Δ cells have different polysome profiles; in *sfp1*Δ cells, the majority of ribosomes are associated with lower-order polysomes (Fingerman et al. 2003), whereas in *gcr1*Δ cells, the overall levels of both higher- and lower-order polysomes are reduced (our unpublished data). The second model proposes an additional function for Gcr1 and/or Sfp1 that influences progression through Start. For Gcr1, this second function may be an effect on *CLN* levels that is independent of its effect on RPGs; consistent with this idea, we have previously observed a reduction in *CLN1* and *CLN2* levels in a *gcr1*Δ *cln3*Δ mutant that is greater than the effect of either *gcr1*Δ or *cln3*Δ alone (Willis et al. 2003). For Sfp1, this second function might be related to its role in DNA damage (Xu and Norris 1998). A variation of this model hypothesizes that although Gcr1 and Sfp1 have similar functions in stimulating RPG expression, yeast cells require those functions at different times during the cell cycle. Indeed, it has previously been suggested that Sfp1 function may be required at the G2/M transition (Xu and Norris 1998) as well as for passage through Start. Discovering which of these two models is correct should be of critical importance in elucidating the delicate balance between growth, RPG expression, and cell cycle progression.

Acknowledgments We thank Kristina Clarke, Nicole Thompson and Baobin Kang for outstanding technical support and other members of the Santangelo lab and USM yeast group for helpful suggestions and comments. This work was supported by a National Institutes of Health Grant RR16476 to G.M.S.

References

Bailey TL, Williams N, Misleh C, Li WW (2006) MEME: discovering and analyzing DNA and protein sequence motifs. Nucleic Acids Res 34:W369–W373

Banuelos M, Fraenkel DG (1982) *Saccharomyces carlsbergensis* fdp mutant and futile cycling of fructose 6-phosphate. Mol Cell Biol 2:921–929

Blumberg H, Silver P (1991) A split zinc-finger protein is required for normal yeast growth. Gene 107:101–110

Brauer MJ, Saldanha AJ, Dolinski K, Botstein D (2005) Homeostatic adjustment and metabolic remodeling in glucose-limited yeast cultures. Mol Biol Cell 16:2503–2517

Brazma A, Hingamp P, Quackenbush J, Sherlock G, Spellman P, Stoeckert C, Aach J, Ansorge W, Ball CA, Causton HC, Gaasterland T, Glenisson P, Holstege FC, Kim IF, Markowitz V, Matese JC, Parkinson H, Robinson A, Sarkans U, Schulze-Kremer S, Stewart J, Taylor R, Vilo J, Vingron M (2001) Minimum information about a microarray experiment (MIAME)-toward standards for microarray data. Nat Genet 29:365–371

Buchman AR, Kimmerly WJ, Rine J, Kornberg RD (1988) Two DNA-binding factors recognize specific sequences at silencers, upstream activating sequences, autonomously replicating sequences, and telomeres in *Saccharomyces cerevisiae*. Mol Cell Biol 8:210–225

Cherel I, Thuriaux P (1995) The *IFH1* gene product interacts with a fork head protein in *Saccharomyces cerevisiae*. Yeast 11:261–270

Cipollina C, Alberghina L, Porro D, Vai M (2005) *SFP1* is involved in cell size modulation in respiro-fermentative growth conditions. Yeast 22:385–399

Clifton D, Fraenkel DG (1981) The *gcr* (glycolysis regulation) mutation of *Saccharomyces cerevisiae*. J Biol Chem 256:13074–13078

Costanzo MC, Hogan JD, Cusick ME, Davis BP, Fancher AM, Hodges PE, Kondu P, Lengieza C, Lew-Smith JE, Lingner C, Roberg-Perez KJ, Tillberg M, Brooks JE, Garrels JI (2000) The yeast proteome database (YPD) and *Caenorhabditis elegans* proteome database (WormPD): comprehensive resources for the organization and comparison of model organism protein information. Nucleic Acids Res 28:73–76

Dabeva MD, Post-Beittenmiller MA, Warner JR (1986) Autogenous regulation of splicing of the transcript of a yeast ribosomal protein gene. Proc Natl Acad Sci USA 83:5854–5857

David L, Huber W, Granovskaia M, Toedling J, Palm CJ, Bofkin L, Jones T, Davis RW, Steinmetz LM (2006) A high-resolution map of transcription in the yeast genome. Proc Natl Acad Sci USA 103:5320–5325

Deminoff SJ, Santangelo GM (2001) Rap1p requires Gcr1p and Gcr2p homodimers to activate ribosomal protein and glycolytic genes, respectively. Genetics 158:133–143

Deminoff SJ, Willis KA, Santangelo GM (2003) Coordination between eukaryotic growth and cell cycle progression: *RAP1*/*GCR1* transcriptional activation mediates glucose-dependent *CLN* function. Recent Res Dev Genet 3:1–16

DeRisi JL, Iyer VR, Brown PO (1997) Exploring the metabolic and genetic control of gene expression on a genomic scale. Science 278:680–686

Fewell SW, Woolford JL Jr (1999) Ribosomal protein S14 of *Saccharomyces cerevisiae* regulates its expression by binding to RPS14B pre-mRNA and to 18S rRNA. Mol Cell Biol 19:826–834

Fingerman I, Nagaraj V, Norris D, Vershon AK (2003) Sfp1 plays a key role in yeast ribosome biogenesis. Eukaryot Cell 2:1061–1068

Gelperin D, Horton L, Beckman J, Hensold J, Lemmon SK (2001) Bms1p, a novel GTP-binding protein, and the related Tsr1p are required for distinct steps of 40S ribosome biogenesis in yeast. RNA 7:1268–1283

Hartwell LH (1974) *Saccharomyces cerevisiae* cell cycle. Bacteriol Rev 38:164–198

Hartwell LH, Culotti J, Pringle JR, Reid BJ (1974) Genetic control of the cell division cycle in yeast. Science 183:46–51

Henry YA, Lopez MC, Gibbs JM, Chambers A, Kingsman SM, Baker HV, Stanway CA (1994) The yeast protein Gcr1p binds to the *PGK* UAS and contributes to the activation of transcription of the *PGK* gene. Mol Gen Genet 245:506–511

Hermann-Le Denmat S, Werner M, Sentenac A, Thuriaux P (1994) Suppression of yeast RNA polymerase III mutations by *FHL1*, a gene coding for a fork head protein involved in rRNA processing. Mol Cell Biol 14:2905–2913

Holmberg S, Schjerling P (1996) Cha4p of *Saccharomyces cerevisiae* activates transcription via serine/threonine response elements. Genetics 144:467–478

Ito T, Chiba T, Ozawa R, Yoshida M, Hattori M, Sakaki Y (2001) A comprehensive two-hybrid analysis to explore the yeast protein interactome. Proc Natl Acad Sci USA 98:4569–4574

Jin SB, Zhao J, Bjork P, Schmekel K, Ljungdahl PO, Wieslander L (2002) Mrd1p is required for processing of pre-rRNA and for maintenance of steady-state levels of 40 S ribosomal subunits in yeast. J Biol Chem 277:18431–18439

Johnston GC, Ehrhardt CW, Lorincz A, Carter BL (1979) Regulation of cell size in the yeast *Saccharomyces cerevisiae*. J Bacteriol 137:1–5

Johnston GC, Pringle JR, Hartwell LH (1977) Coordination of growth with cell division in the yeast *Saccharomyces cerevisiae*. Exp Cell Res 105:79–98

Jorgensen P, Nishikawa JL, Breitkreutz BJ, Tyers M (2002) Systematic identification of pathways that couple cell growth and division in yeast. Science 297:395–400

Jorgensen P, Rupes I, Sharom JR, Schneper L, Broach JR, Tyers M (2004) A dynamic transcriptional network communicates growth potential to ribosome synthesis and critical cell size. Genes Dev 18:2491–2505

Kief DR, Warner JR (1981) Coordinate control of syntheses of ribosomal ribonucleic acid and ribosomal proteins during nutritional shift-up in *Saccharomyces cerevisiae*. Mol Cell Biol 1:1007–1015

Krogan NJ, Cagney G, Yu H, Zhong G, Guo X, Ignatchenko A, Li J, Pu S, Datta N, Tikuisis AP, Punna T, Peregrin-Alvarez JM, Shales M, Zhang X, Davey M, Robinson MD, Paccanaro A, Bray JE, Sheung A, Beattie B, Richards DP, Canadien V, Lalev A, Mena F, Wong P, Starostine A, Canete MM, Vlasblom J, Wu S, Orsi C, Collins SR, Chandran S, Haw R, Rilstone JJ, Gandi K, Thompson NJ, Musso G, St Onge P, Ghanny S, Lam MH, Butland G, Altaf-Ul AM, Kanaya S, Shilatifard A, O'Shea E, Weissman JS, Ingles CJ, Hughes TR, Parkinson J, Gerstein M, Wodak SJ, Emili A, Greenblatt JF (2006) Global landscape of protein complexes in the yeast *Saccharomyces cerevisiae*. Nature 440:637–643

Lee TI, Rinaldi NJ, Robert F, Odom DT, Bar-Joseph Z, Gerber GK, Hannett NM, Harbison CT, Thompson CM, Simon I, Zeitlinger J, Jennings EG, Murray HL, Gordon DB, Ren B, Wyrick JJ, Tagne JB, Volkert TL, Fraenkel E, Gifford DK, Young RA (2002) Transcriptional regulatory networks in *Saccharomyces cerevisiae*. Science 298:799–804

Li B, Vilardell J, Warner JR (1996) An RNA structure involved in feedback regulation of splicing and of translation is critical for biological fitness. Proc Natl Acad Sci USA 93:1596–1600

Li Z, Paulovich AG, Woolford JL Jr (1995) Feedback inhibition of the yeast ribosomal protein gene *CRY2* is mediated by the nucleotide sequence and secondary structure of *CRY2* premRNA. Mol Cell Biol 15:6454–6464

Lieb JD, Liu X, Botstein D, Brown PO (2001) Promoter-specific binding of Rap1 revealed by genome-wide maps of protein-DNA association. Nat Genet 28:327–334

Lodi T, Donnini C, Ferrero I (1991) Catabolite repression by galactose in overexpressed *GAL4* strains of *Saccharomyces cerevisiae*. J Gen Microbiol 137:1039–1044

Lopez MC, Baker HV (2000) Understanding the growth phenotype of the yeast *gcr1* mutant in terms of global genomic expression patterns. J Bacteriol 182:4970–4978

Lu J, Kobayashi R, Brill SJ (1996) Characterization of a high mobility group 1/2 homolog in yeast. J Biol Chem 271:33678–33685

MacIsaac KD, Wang T, Gordon DB, Gifford DK, Stormo GD, Fraenkel E (2006) An improved map of conserved regulatory sites for *Saccharomyces cerevisiae*. BMC Bioinformatics 7:113

Mager WH, Planta RJ (1991) Coordinate expression of ribosomal protein genes in yeast as a function of cellular growth rate. Mol Cell Biochem 104:181–187

Measday V, Moore L, Ogas J, Tyers M, Andrews B (1994) The *PCL2* (*ORFD*)-PHO85 cyclin-dependent kinase complex: a cell cycle regulator in yeast. Science 266:1391–1395

Menon BB, Sarma NJ, Pasula S, Deminoff SJ, Willis KA, Barbara KE, Andrews B, Santangelo GM (2005) Reverse recruitment: the Nup84 nuclear pore subcomplex mediates Rap1/Gcr1/Gcr2 transcriptional activation. Proc Natl Acad Sci USA 102:5749–5754

Mizuta K, Warner JR (1994) Continued functioning of the secretory pathway is essential for ribosome synthesis. Mol Cell Biol 14:2493–2502

Nash R, Tokiwa G, Anand S, Erickson K, Futcher AB (1988) The *WHI1*+ gene of *Saccharomyces cerevisiae* tethers cell division to cell size and is a cyclin homolog. EMBO J 7:4335–4346

Parviz F, Heideman W (1998) Growth-independent regulation of *CLN3* mRNA levels by nutrients in *Saccharomyces cerevisiae*. J Bacteriol 180:225–230

Polakis ES, Bartley W (1965) Changes in the enzyme activities of *Saccharomyces cerevisiae* during aerobic growth on different carbon sources. Biochem J 97:284–297

Polakis ES, Bartley W (1966) Changes in the intracellular concentrations of adenosine phosphates and nicotinamide nucleotides during the aerobic growth cycle of yeast on different carbon sources. Biochem J 99:521–533

Popolo L, Vanoni M, Alberghina L (1982) Control of the yeast cell cycle by protein synthesis. Exp Cell Res 142:69–78

Prescott EM, Osheim YN, Jones HS, Alen CM, Roan JG, Reeder RH, Beyer AL, Proudfoot NJ (2004) Transcriptional termination by RNA polymerase I requires the small subunit Rpa12p. Proc Natl Acad Sci USA 101:6068–6073

Presutti C, Ciafre SA, Bozzoni I (1991) The ribosomal protein L2 in *S. cerevisiae* controls the level of accumulation of its own mRNA. EMBO J 10:2215–2221

Robinson MD, Grigull J, Mohammad N, Hughes TR (2002) FunSpec: a web-based cluster interpreter for yeast. BMC Bioinformatics 3:35

Samanta MP, Tongprasit W, Sethi H, Chin CS, Stolc V (2006) Global identification of noncoding RNAs in *Saccharomyces cerevisiae* by modulating an essential RNA processing pathway. Proc Natl Acad Sci USA 103:4192–4197

Santangelo GM (2006) Glucose signaling in *Saccharomyces cerevisiae*. Microbiol Mol Biol Rev 70:253–282

Santangelo GM, Tornow J (1990) Efficient transcription of the glycolytic gene *ADH1* and three translational component genes requires the *GCR1* product, which can act through *TUF*/*GRF*/*RAP* binding sites. Mol Cell Biol 10:859–862

Sasaki H, Uemura H (2005) Influence of low glycolytic activities in *gcr1* and *gcr2* mutants on the expression of other metabolic pathway genes in *Saccharomyces cerevisiae*. Yeast 22:111–127

Sherman F (2002) Getting started with yeast. Methods Enzymol 350:3–41

Slonim DK (2002) From patterns to pathways: gene expression data analysis comes of age. Nat Genet 21:5–9

Southern E, Mir K, Shchepinov M (1999) Molecular interactions on microarrays. Nat Genet 21:5–9

Stoppani AO (1951) Pyruvate metabolism in *Saccharomyces cerevisiae*. Nature 167:653–654

Tokiwa G, Tyers M, Volpe T, Futcher B (1994) Inhibition of G1 cyclin activity by the Ras/cAMP pathway in yeast. Nature 371:342–345

Tornow J, Zeng X, Gao W, Santangelo GM (1993) *GCR1*, a transcriptional activator in *Saccharomyces cerevisiae*, complexes with *RAP1* and can function without its DNA binding domain. EMBO J 12:2431–2437

Tsuno A, Miyoshi K, Tsujii R, Miyakawa T, Mizuta K (2000) *RRS1*, a conserved essential gene, encodes a novel regulatory protein required for ribosome biogenesis in *Saccharomyces cerevisiae*. Mol Cell Biol 20:2066–2074

Turkel S, Turgut T, Lopez MC, Uemura H, Baker HV (2003) Mutations in *GCR1* affect *SUC2* gene expression in *Saccharomyces cerevisiae*. Mol Genet Genomics 268:825–831

Wang Y, Pierce M, Schneper L, Guldal CG, Zhang X, Tavazoie S, Broach JR (2004) Ras and Gpa2 mediate one branch of a redundant glucose signaling pathway in yeast. PLoS Biol 2:610–622

Warner JR (1999) The economics of ribosome biosynthesis in yeast. Trends Biochem Sci 24:437–440

Wegierski T, Billy E, Nasr F, Filipowicz W (2001) Bms1p, a G-domain-containing protein, associates with Rcl1p and is required for 18S rRNA biogenesis in yeast. RNA 7:1254–1267

Willis KA, Barbara KE, Menon BB, Moffat J, Andrews B, Santangelo GM (2003) The global transcriptional activator of *Saccharomyces cerevisiae*, Gcr1p, mediates the response to glucose by stimulating protein synthesis and *CLN*-dependent cell cycle progression. Genetics 165:1017–1029

Wu K, Wu P, Aris JP (2001) Nucleolar protein Nop12p participates in synthesis of 25S rRNA in *Saccharomyces cerevisiae*. Nucleic Acids Res 29:2938–2949

Wu LF, Hughes TR, Davierwala AP, Robinson MD, Stoughton R, Altschuler SJ (2002) Large-scale prediction of *Saccharomyces cerevisiae* gene function using overlapping transcriptional clusters. Nat Genet 31:255–265

Xu Z, Norris D (1998) The *SFP1* gene product of *Saccharomyces cerevisiae* regulates G2/M transitions during the mitotic cell cycle and DNA-damage response. Genetics 150:1419–1428

Zeng X, Deminoff SJ, Santangelo GM (1997) Specialized Rap1p/Gcr1p Transcriptional Activation Through Gcr1p DNA Contacts Requires Gcr2p, as Does Hyperphosphorylation of Gcr1p. Genetics 147:493–505

Zhu J, Zhang MQ (1999) SCPD: a promoter database of the yeast *Saccharomyces cerevisiae*. Bioinformatics 15:607–611